NASA TN D-16

TECHNICAL NOTE
D-16

LOW-SPEED WIND-TUNNEL INVESTIGATION OF BLOWING BOUNDARY-LAYER CONTROL ON LEADING- AND TRAILING-EDGE FLAPS OF A FULL-SCALE, LOW-ASPECT-RATIO, 42° SWEPT-WING AIRPLANE CONFIGURATION

By Ralph L. Maki and Demo J. Giulianetti

Ames Research Center
Moffett Field, Calif.

NATIONAL AERONAUTICS AND SPACE ADMINISTRATION

WASHINGTON

August 1959

NATIONAL AERONAUTICS AND SPACE ADMINISTRATION

TECHNICAL NOTE D-16

LOW-SPEED WIND-TUNNEL INVESTIGATION OF BLOWING BOUNDARY-LAYER CONTROL ON LEADING- AND TRAILING-EDGE FLAPS OF A FULL-SCALE, LOW-ASPECT-RATIO, 42° SWEPT-WING AIRPLANE CONFIGURATION

By Ralph L. Maki and Demo J. Giulianetti

SUMMARY

A wind-tunnel investigation was made on a complete full-scale model having a thin, low-aspect-ratio, 42° sweptback wing with single- and double-droop leading-edge flaps and trailing-edge flaps, both equipped with blowing boundary-layer control (BLC). Lift, drag, pitching-moment, and rolling-moment data were measured for an angle-of-attack range from -8° through stall at a Reynolds number of 8.1 million.

The effects of leading-edge flap deflection and blowing BLC on lift and the delay of leading-edge flow separation were generally similar to those reported in previous investigations (NACA RM A58A09 and NASA MEMO 1-23-59A) for wings of similar sweep and aspect ratio. These effects should be qualitatively applicable to other models of similar wing plan form.

Leading-edge flap deflections up to 40° without BLC resulted in increases in maximum lift because flow separation at the wing leading edge was delayed to higher angles of attack. For deflections greater than 40°, moderate amounts of leading-edge blowing BLC were required to prevent the flow from separating over the flap knee; with BLC applied, maximum lift continued to increase with increasing flap deflection up to 60°. With the leading-edge flaps deflected 60° from 0.4 to 1.0 semispan and with blowing BLC applied over this span extent, the deflection inboard of 0.4 semispan could be reduced to 40° with little loss in maximum lift. With this leading-edge configuration (blowing momentum coefficient of 0.02) and with trailing-edge flaps deflected 40° with a blowing momentum coefficient of 0.009, the maximum lift coefficient was 1.72 at 20° angle of attack. With full-span leading-edge flaps deflected 40° without BLC and the same trailing-edge flap configuration with BLC, the maximum lift coefficient was 1.41 and occurred at 12° angle of attack.

Double-droop leading-edge flap configurations were compared with single-droop leading-edge flap configurations without BLC and were also tested in conjunction with partial-span single-droop flaps with BLC applied. In no case was double droop significantly more effective than single droop.

The model with leading- and trailing-edge flaps deflected with blowing BLC applied was longitudinally stable for many configurations for the angle-of-attack range up to and beyond stall; however, instability occurred at maximum lift for a small angle-of-attack range for some of the configurations.

Tests were made to determine the effects of blocking the flow through the trailing-edge flap nozzle by means of various arrangements and sizes of plugs which blocked as high as 22.4 percent of the nozzle span. Small losses in lift resulted for trailing-edge flaps deflected 40° and larger losses in lift when deflected 55°. Sizable losses in roll control power due to nozzle blockage occurred with the flaps differentially deflected as ailerons about an average flap deflection of 40°.

INTRODUCTION

Studies have been made on the use of BLC as a means of increasing lift and delaying stall on many wing-body combinations. Investigations of both area-suction and blowing trailing-edge flaps showed that flap effectiveness was improved at high flap deflections. The gains in flap lift, however, were often limited to low angles of attack because of separation at the leading edge of thin, low-aspect-ratio, sweptback wings. Investigations employing leading-edge devices in conjunction with blowing BLC trailing-edge flaps have shown delays in leading-edge air-flow separation to higher angles of attack and large increases in maximum lift. Studies of models using leading-edge BLC flaps, (refs. 1 to 4) have shown them to be a highly effective means for leading-edge stall control.

The present investigation was made on a complete airplane model having an aspect-ratio-3.4 wing with 42° sweepback of the quarter-chord line and mounted high on the fuselage at positive incidence. The purpose of the study was to determine the extent of increases in lift resulting from the use of various leading-edge flap deflections with and without blowing BLC, in combination with blowing trailing-edge flaps. Brief tests of doubly drooped leading-edge flaps without BLC were made. Other objectives of the study were to determine the effects of blocking the flow through the trailing-edge nozzle on lift with flaps symmetrically deflected, and on roll control with flaps differentially deflected as ailerons.

The investigation was conducted in the low-speed, full-scale, 40- by 80-foot wind tunnel of the Ames Research Center at a Reynolds number of 8.1×10^{6}.

NOTATION

BLC	boundary-layer control
b	wing span, ft
c	wing chord, measured parallel to the plane of symmetry, ft
$\bar{c}$	mean aerodynamic chord, $\frac{\int_0^{b/2} c^2 dy}{\int_0^{b/2} c\, dy}$, ft
C_L	lift coefficient
C_D	drag coefficient
C_m	pitching-moment coefficient (location of moment center defined in fig. 1)
C_μ	blowing momentum coefficient, $\frac{WV_j}{gq_\infty S}$
g	gravitational acceleration, ft/sec^2
i_t	horizontal-tail incidence, deg
i_w	wing incidence, deg
p	static pressure, lb/sq ft
p_∞	free-stream static pressure, lb/sq ft
P_t	total pressure, lb/sq ft
q_∞	free-stream dynamic pressure, lb/sq ft
R	universal gas constant for air, and Reynolds number, $\frac{V_\infty \bar{c}}{\nu}$
S	wing area, sq ft
T	absolute total temperature, $^\circ$R
V_j	jet velocity at blowing BLC nozzle, ft/sec $\sqrt{\frac{2\gamma}{\gamma-1} gRT_D \left[1 - \left(\frac{p_\infty}{P_{t_D}}\right)^{\frac{\gamma-1}{\gamma}}\right]}$,
V_∞	free-stream velocity, ft/sec
W	weight rate of flow of air, lb/sec

y	spanwise distance normal to fuselage center line, ft
α	angle of attack referred to fuselage center line, deg
γ	ratio of specific heats for air
Δ	incremental value
δ	flap deflection, measured normal to hinge line, deg
η	fraction semispan, $\frac{2y}{b}$
ν	kinematic viscosity, ft^2/sec

Subscripts

D	flap duct
f	trailing-edge flap
i	inboard trailing-edge flap
L	left
max	maximum
N	leading-edge flap
o	outboard trailing-edge flap
R	right
T	wind-tunnel wall interference

Example of Leading-Edge Flap Deflection Notation

40-60-60	inboard flap segment deflected 40°, middle flap segment deflected 60°, and outboard flap segment deflected 60°, respectively (Unless otherwise noted, leading-edge flap deflections are for the forward flap undeflected with respect to the aft flap.)

MODEL AND APPARATUS

The model was a complete, full-scale, fighter-type airplane model having an aspect-ratio-3.4 wing with 42° sweepback of the quarter-chord line. The wing was mounted high on the fuselage and was equipped with a variable incidence device. The majority of tests were run with the wing at a positive incidence of 4.5°. The wing leading edge had a chord extension of 12 percent of the basic chord extending from 0.63 to 1.0 semispan. Dimensional data of the model are listed in table I. A three-view sketch of the model is shown in figure 1. Figure 2 is a photograph of the model in the test section of the wind tunnel.

Leading-Edge Flaps

Single- and double-droop flaps were provided at the leading edge of the wing and were hinged on the lower surface at 6- and 15-percent chord (fig. 3(a)). The flaps were in three spanwise sections; the inboard section (0.12 to 0.42 b/2), the middle section (0.42 to 0.63 b/2), and the outboard section (0.63 to 1.0 b/2). The blowing nozzle was located on the 15-percent-chord flap hinge radius with the blowing air directed over the knee of the flap as shown in figure 3(a). The nozzle gap was set at 0.026 inch by means of wire of the appropriate diameter formed into washers and held in place by screws set on 2-1/2-inch centers. The screws and wire washers blocked approximately 11 percent of the nozzle area. Blowing was applied from 0.42 to 1.0 semispan.

Trailing-Edge Flaps

The trailing-edge flaps were in two spanwise sections; the inboard section (0.13 to 0.22 b/2) and the outboard section (0.22 to 0.63 b/2). Flap deflections from 0° to 55° were provided. The blowing nozzle was located in the flap as shown in figure 3(b) and extended over the entire flap span. The nozzle gap was set at 0.026 inch in the same manner as described for the leading-edge flap nozzle. The screws and wire washers in the nozzle blocked approximately 8 percent of the nozzle area. For some tests additional blockage of the flow through the trailing-edge nozzle was obtained by means of plugs of various lengths.

Horizontal Tail

The horizontal tail was mounted low on the model (see table I) and was of aspect ratio 3.4 with 45° sweepback of the quarter-chord line.

Tail incidence was maintained at 0° for the majority of tests. A few tests were made with the horizontal tail off.

High-Pressure BLC Air Source

Two Westinghouse J-34 turbojet engines were installed in the fuselage and compressor air bleed from the last stage of compression was used as the source of compressed air for the blowing BLC systems. The amount of bleed air delivered to the nozzles was determined from static and total pressure and temperature measurements at suitable measuring stations in the ducts which were calibrated against a standard thin-plate orifice.

Thrust

The engine thrust was determined from static thrust calibrations by means of the wind-tunnel balance system and total-pressure measurements at the exit of the tail pipe for each engine.

TESTS

The force and moment data were obtained on the wind-tunnel six-component balance system. Lift, drag, pitching moment, and rolling moment were measured through an angle-of-attack range of -8° through stall and at a Reynolds number of 8.1×10^6 based on the wing mean aerodynamic chord which corresponds to a free-stream dynamic pressure of about 15 pounds per square foot.

Various arrangements of single- and double-droop flap deflections from 0° to 60° on the inboard, middle, and outboard sections of the leading-edge were tested with and without blowing BLC. Data were recorded for leading-edge blowing momentum coefficients up to a maximum of 0.021. Leading-edge blowing BLC was restricted to the region 0.42 to 1.0 b/2.

Trailing-edge flap deflections of 40° and 55° were tested with blowing BLC applied at these deflections. The majority of data was obtained for a constant flap blowing momentum coefficient of about 0.009.

The flow through the trailing-edge blowing nozzle was blocked by means of nozzle plugs ranging in length from 1 to 11.3 inches. Various combinations of these plugs were tested which represented nozzle blockages as great as 22.4 percent. The effects of nozzle blockage on roll control power were investigated and data are presented for differentially

deflected flaps, acting as ailerons, of 50° and 30° on the left and right semispans, respectively.

The data for most of the tests are for the model with the wing at a positive incidence of 4.5° and the horizontal tail at 0° incidence. Unless otherwise noted the data are for the model with the horizontal tail on.

CORRECTIONS

The data have been corrected for stream angle inclination and wind-tunnel wall interference. The following corrections for wind-tunnel wall interference were applied to the data:

$$\alpha_T = 1.20\ C_L$$

$$C_{D_T} = 0.021\ C_L^2$$

$$C_{m_T} = 0.010\ C_L \text{ (horizontal tail on only)}$$

No corrections were made for interference of the model support struts. Jet engine thrust effects have been removed from the lift, drag, and pitching-moment data.

RESULTS

The primary purpose of this study was to determine the effects of leading-edge flap deflection, especially with blowing BLC applied to the leading-edge flaps, on the longitudinal characteristics of the model with trailing-edge flaps deflected with blowing BLC. Results summarizing these effects are presented in figures 4 to 7 and will be discussed first. A brief study of full-span, doubly deflected, leading-edge flaps without BLC was made and the results, in tabular form, are compared with those for singly deflected leading-edge flaps. The effects of discontinuities in the blowing BLC system along the span of the trailing-edge nozzles were studied. The effects of these discontinuities on lift with symmetrically deflected flaps (fig. 8) and on roll control power with flaps differentially deflected as ailerons (figs. 9 and 10) are discussed. Additional lift, drag, and pitching-moment data for various model configurations are presented without discussion in figures 11 to 14.

DISCUSSION

General Effects of Leading- and Trailing-Edge Flap Deflection and BLC

This is the third in a series of studies of leading-edge flap blowing BLC made at the Ames Research Center 40- by 80-foot wind tunnel on swept wing designs suitable for fighter or interceptor use. (The work of refs. 1 and 2 precedes this study.) Similarities of the present results with those of the previous investigations will be noted in the course of the discussion.

Effects of trailing-edge flap deflection with BLC.- Trailing-edge flap deflections of 40° and 55° with blowing BLC gave sizable lift increments at low angles of attack (fig. 4). The variations of lift with $C_{\mu f}$ for these flap deflections are shown in figure 5. Observation of tufts and surface pressure measurements showed that sufficient blowing BLC was used to maintain attached flow for the data with 40° deflection at angles of attack up to those for maximum lift, but that insufficient blowing BLC for flow attachment was used for the data with 55° deflection. The data shown in figure 5 indicate the lack of complete flow attachment for flaps deflected 55° at $\alpha = 14.1^\circ$.

With trailing-edge flaps deflected 40° and the leading-edge flaps undeflected, the flap lift increment diminishes above about 5° angle of attack (fig. 4(a)). References 1 and 2 also report losses of flap lift at moderate angles of attack. Figure 4(a) shows that an increased rate of rise of C_D and severe pitching-moment changes accompany the loss of flap lift. These effects result from the occurrence of flow separation near the wing leading edge.

Effects of leading-edge flap deflection without BLC.- Deflecting the leading-edge flaps 40° delayed leading-edge flow separation to about 12° angle of attack with trailing-edge flaps deflected 40° with BLC (fig. 4(a)). This resulted in an increase in maximum lift to 1.4 (a $C_{L_{max}}$ increment of about 0.3 over that measured with leading-edge flaps undeflected). Flow separation was observed to occur on the outboard section of the wing near the leading edge, that is, forward of the flap hinge radius or knee. With the leading-edge flaps deflected 60° from 0.4 to 1.0 semispan (fig. 4(a)), the flow separated over the flap knee (in the region of adverse pressure gradient) at approximately the same spanwise position. This resulted in a large loss in maximum lift as compared with the 40° leading-edge flap deflection. The data presented in figure 6 indicate that, with respect to $C_{L_{max}}$, the optimum full-span leading-edge flap deflection without BLC is about 40°. For the model reported in reference 1 the highest value of $C_{L_{max}}$ for configurations without leading-edge BLC was measured with the leading-edge flaps deflected 0-40-50.

Effects of leading-edge flap BLC.- A large gain in $C_{L_{max}}$ was obtained with the application of a small amount of blowing ($C_{\mu_N} = 0.005$) over the flap knee with the leading-edge flaps deflected 60° from 0.4 semispan to the wing tip (fig. 4(a)). When C_{μ_N} was increased to 0.021 (the maximum for these tests), $C_{L_{max}}$ increased to 1.72 at about 20° angle of attack. Another example of the large values of $C_{L_{max}}$ obtainable with highly deflected leading-edge flaps with BLC is shown in figure 6 where the data for $C_{\mu_N} = 0.019$ with a full-span flap deflection of 60° lies on a line which is very nearly a linear extension of the curve through the low-deflection data. With trailing-edge flaps deflected 55° with BLC (fig. 4(b)) gains in $C_{L_{max}}$ with increasing C_{μ_N} are apparent although the value of C_{μ_f} (0.009) is considerably less than that required for complete flow attachment (see fig. 5).

Variations of $C_{L_{max}}$ with C_{μ_N} are shown in figure 7 for several wing leading-edge configurations. The rapid rise of C_L when C_{μ_N} is increased from 0 to about 0.0006 results from the elimination of flow separation over the flap knee. The moderate rate of rise of $C_{L_{max}}$ as C_{μ_N} is further increased results from the delay of flow separation occurring forward of the flap knee near the wing leading edge. The initial rapid rise of $C_{L_{max}}$ and subsequent moderate rise also appear in the data presented in reference 1.

Effects of spanwise distribution of δ_N.- Several variations in spanwise distribution of leading-edge flap deflection are represented in the data presented in figure 7. Although no attempt was made to determine an optimum leading-edge configuration, the data shown point out two features of interest. Maximum lift was not affected by changes from 40° to 60° deflection of the inboard flap segments. However, $C_{L_{max}}$ was decreased by about 0.12, for all values of C_{μ_N} above about 0.006, when the deflection of the middle flap segment was reduced from 60° to 40°. These results are qualitatively similar to the results reported in references 1 to 4, that is, deflections inboard of some critical spanwise position can be reduced with little effect on $C_{L_{max}}$. In references 3 and 4, the effects of spanwise distribution of both deflection and blowing BLC were studied in detail in an attempt to optimize the leading-edge configuration.

Lift Effectiveness of Single- and Double-Droop Leading-Edge Flaps Without BLC

It has been shown (figs. 4 and 6) that single-droop leading-edge flaps are effective at deflections up to 40° in delaying the onset of flow separation near the wing leading edge. This occurs because the negative pressure peak near the leading edge is reduced (at constant α) as the leading-edge flap is deflected, and the pressure recovery occurs largely over the flap knee, that is, in a region of less curvature than

at the leading edge. For deflections greater than 40°, the negative pressure peak and recovery gradient over the flap knee become critical, and flow separation first appears in this region. It was reasoned that a doubly hinged flap might further reduce the peak negative pressures and the pressure gradients at constant α, hence allow higher total flap deflections to be effective in delaying flow separation to even higher angles of attack.

The double-droop flaps installed on the model to explore this idea were hinged at 6- and 15-percent chord. Only deflections totaling more than 40° were tested. Values of $C_{L_{max}}$ measured for three double-droop configurations are compared in the following table with the value measured for a single-droop deflection of 40°. Trailing-edge flaps were deflected 40° in all cases and C_{μ_f} was about 0.009.

	Double droop			Single droop
δ_N, deg, forward flap	40-40-40	40-40-40	40-40-45	
δ_N, deg, aft flap	10-10-15	10-10-20	10-10-15	40-40-40
$C_{L_{max}}$	1.42	1.43	1.38	1.40

The double-droop flap tests were too limited to draw any general conclusions. However, it is obvious that double droop as tested did not significantly increase maximum lift as compared with the single-droop configuration with less total deflection. During the tests of double-droop flaps, it was observed that the onset of flow separation changed from a position near the wing leading edge to the region over the flap knee when the deflection of the outboard forward flap was increased from 40° to 45°. This change in the nature of initial flow separation was previously observed to occur when the single-droop flap deflection was increased from 40° to 60° over the outboard region of the wing. Thus, 40° deflection appears to be near the optimum deflection for both the forward and aft flaps, and additional deflection of the aft flap in conjunction with optimum deflection of the forward flap does not materially affect maximum lift.

Effects of Trailing-Edge-Flap Nozzle Blockage

The installation of blowing BLC ducts and nozzles in wings may interfere with hinge attachments and actuators which normally occupy the same area. As a result, for very thin wings it may be necessary to block the blowing nozzle at such points along the nozzle span. Little large-scale data showing the effect of such blockage exists (refs. 5 and 6

present some data). Several portions of the nozzle span were blocked on this model. The results are presented in figures 8 to 10. The values of percent nozzle blockage given in the figures apply to the plugs only; the balance of the "open" nozzle span in each case has the 8-percent blockage due to screws and wire washers as described earlier in the report.

The effects of nozzle blockage on C_L for flaps deflected 40° and 55° are shown in figure 8. There was little loss in C_L with 10.3-percent nozzle blockage and flaps deflected 40°. However, the losses were much more pronounced with flaps deflected 55°. With 22.4-percent blockage the lift is very nearly the same for 40° and 55° trailing-edge flap deflection. As in previous tests, the value of C_{μ_f} with trailing-edge flaps deflected 55° was less than required for complete flow attachment.

The effect of nozzle blockage was also studied for flaps deflected 40° with aileron deflection superposed. To determine the roll control available, tests were made without nozzle blockage for several aileron deflections with and without BLC. These results, given in figure 9, show that the roll control power was approximately doubled by application of blowing BLC. The effects of nozzle blockage were measured with 20° total aileron deflection; the results are shown in figure 10. Sizable losses in roll control power occurred for nozzle plugs more than 1 inch in length. For the same percent blockage fewer plugs of longer length showed more serious effects than more plugs each of shorter length. With 22.4-percent blockage the C_l available (fig. 10) at 0° angle of attack (C_L about 0.8) was about the same as measured with BLC off (fig. 9).

CONCLUSIONS

The following conclusions have been made from the examination of results of this investigation.

1. Leading-edge flap deflections up to about 40° without boundary-layer control (BLC) delay the onset of leading-edge air-flow separation to higher angles of attack.

2. For leading-edge flap deflections greater than 40°, moderate amounts of leading-edge blowing BLC are required to prevent the flow from separating over the flap knee. Large initial increases in maximum lift result from application of small amounts of BLC. Smaller increases in maximum lift are obtained with further increases in blowing.

3. With BLC applied, maximum lift continues to increase with increasing leading-edge flap deflection up to 60°. The flap may be deflected less over the inboard region of the wing than over the outboard region with little effect on maximum lift.

4. With leading-edge flaps deflected and BLC applied, longitudinal stability was maintained to lift coefficients approaching maximum lift. However, instability occurred at maximum lift for a small angle-of-attack range for some configurations.

5. Double-droop leading-edge flaps without BLC were not significantly more effective than single-droop flaps without BLC for increasing maximum lift.

6. With various arrangements of plugs blocking as much as 22.4 percent of the trailing-edge flap nozzle span, small losses in lift resulted for trailing-edge flaps deflected 40°; larger losses resulted with 55° deflection. Consequently, with the flaps deflected differentially as ailerons about a deflection of 40° as flaps, sizable losses in roll control power occurred for more than 3.5 percent blockage.

Results reported in NACA RM A58A09 and NASA MEMO 1-23-59A, for different airplane models with wings of similar sweep and aspect ratio, show that conclusions 1 through 4 are valid for other models of similar plan form.

Ames Research Center
National Aeronautics and Space Administration
Moffett Field, Calif., Mar. 25, 1959

REFERENCES

1. Hickey, David H., and Aoyagi, Kiyoshi: Large-Scale Wind-Tunnel Tests of an Airplane Model With a 45° Sweptback Wing of Aspect Ratio 2.8 Employing High-Velocity Blowing Over the Leading- and Trailing-Edge Flaps. NACA RM A58A09, 1958.

2. Maki, Ralph L.: Low-Speed Wind-Tunnel Investigation of Blowing Boundary-Layer Control on Leading- and Trailing-Edge Flaps of a Large-Scale, Low-Aspect-Ratio, 45° Swept-Wing Airplane Configuration. NASA MEMO 1-23-59A, 1959.

3. Fink, Marvin P., and McLemore, H. Clyde: High-Pressure Blowing Over Flap and Wing Leading Edge of a Thin Large-Scale 49° Swept Wing-Body-Tail Configuration in Combination with a Drooped Nose and a Nose with a Radius Increase. NACA RM L57D23, 1957.

4. McLemore, H. Clyde: Aerodynamic Characteristics in Sideslip of a Large-Scale 49° Sweptback Wing-Body-Tail Configuration with Blowing Applied Over the Flaps and Wing Leading Edge. NASA MEMO 10-11-58L, 1958.

5. Tolhurst, William H., Jr.: Full-Scale Wind-Tunnel Tests of a 35° Sweptback-Wing Airplane With Blowing From the Shroud Ahead of the Trailing-Edge Flaps. NACA TN 4283, 1958.

6. Kelly, Mark W., and Tolhurst, William H., Jr.: Full-Scale Wind-Tunnel Tests of a 35° Sweptback Wing Airplane with High-Velocity Blowing Over the Trailing-Edge Flaps. NACA RM A55I09, 1955.

TABLE I.- DIMENSIONAL DATA OF THE MODEL

Wing	
Area, sq ft	375
Span, ft	35.7
Aspect ratio	3.4
Taper ratio	0.25
Sweep of the quarter chord, deg	42
Dihedral, deg	-5
Chord, streamwise, in.	
Root	202
Tip (without chord extension)	49.9
Mean aerodynamic	141.4
Airfoil section, streamwise	
Root	NACA 65A006
Tip	NACA 65A005 (modified)
Leading-edge flaps	
Single-droop, percent chord	0 to 15
Double-droop, percent chord	
Forward flap	0 to 6
Aft flap	6 to 15
Span, percent semispan	
Inboard	12 to 42
Middle	42 to 63
Outboard	63 to 100
Trailing-edge flaps	
Span, percent semispan	
Inboard	13 to 22
Outboard	22 to 63
Chord, in.	
At 13-percent semispan	41.8
At 22-percent semispan	39.3
At 63-percent semispan	29.9
Horizontal tail	
Area, sq ft	72.3
Span, ft	15.9
Aspect ratio	3.5
Taper ratio	0.3
Sweep of the quarter chord, deg	45
Dihedral, deg	5.3
Chord, streamwise, in.	
Root	83.9
Tip	25.2
Mean aerodynamic	65.4
Tail volume	0.28
Height below extended wing-chord plane, ft (with wing at $+4.5^{\circ}$ incidence and tail at 0° incidence)	3.6

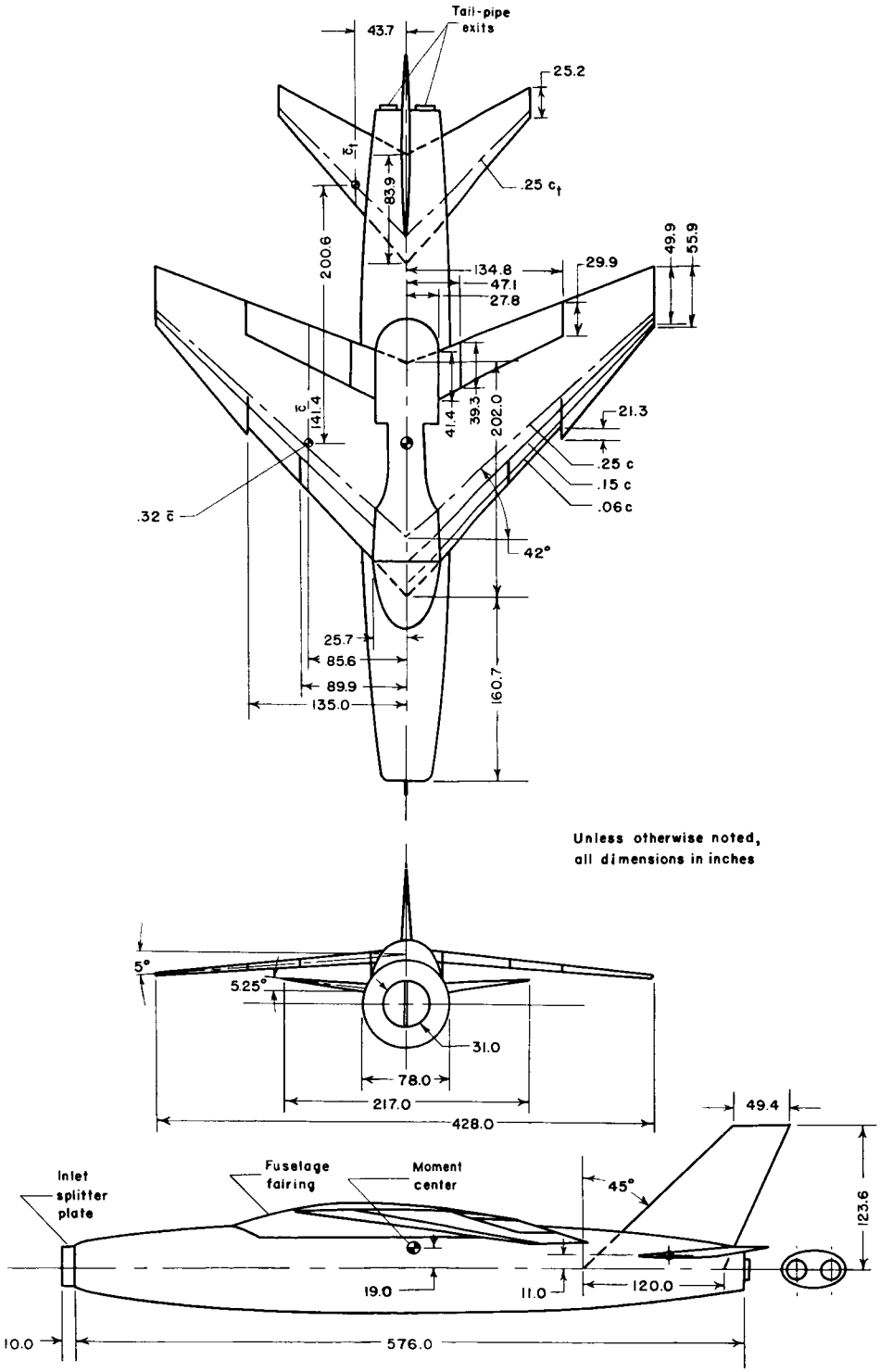

Figure 1.- Geometric details of the model.

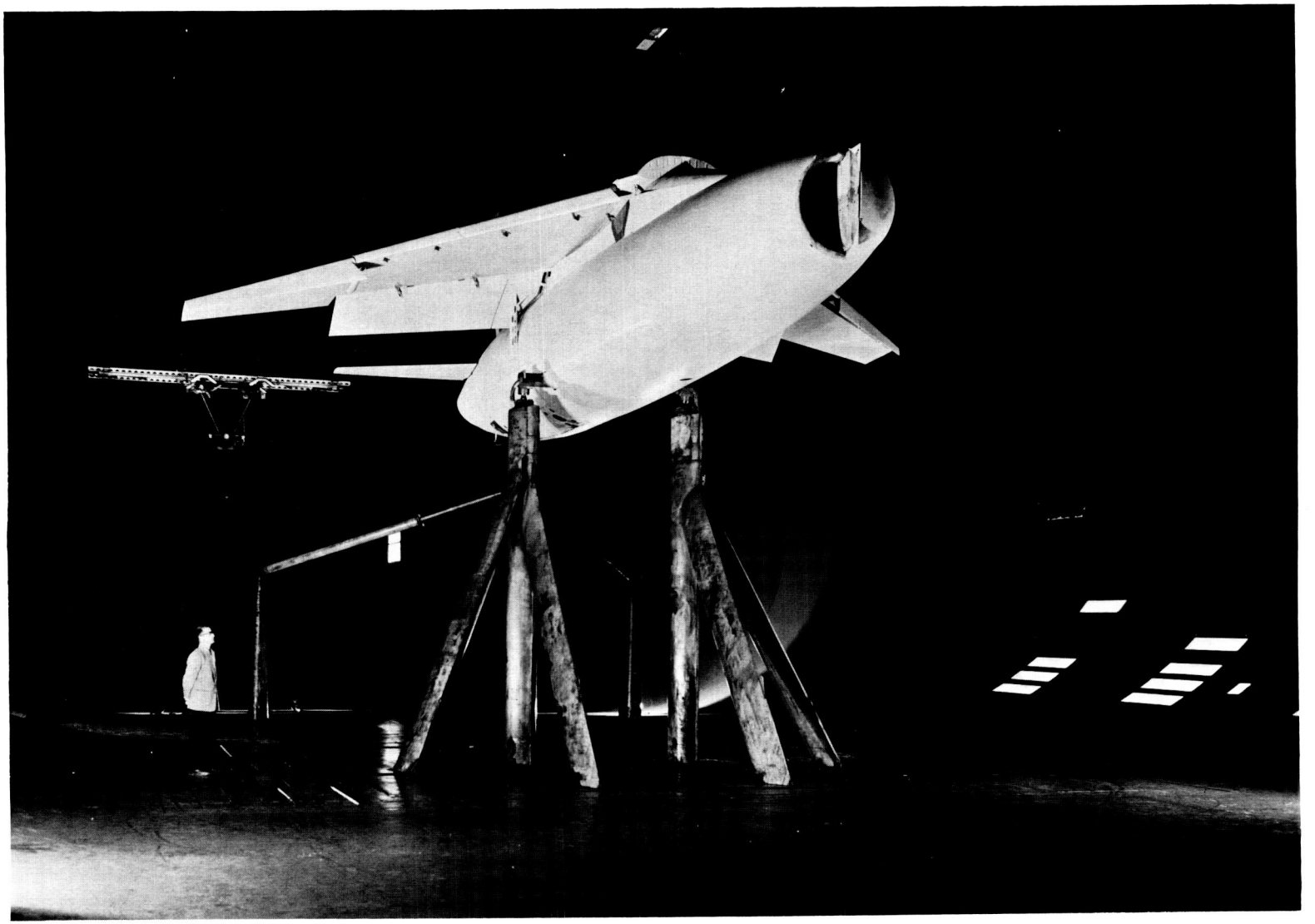

Figure 2.- View of the model mounted in the test section of the wind tunnel.

A-23318

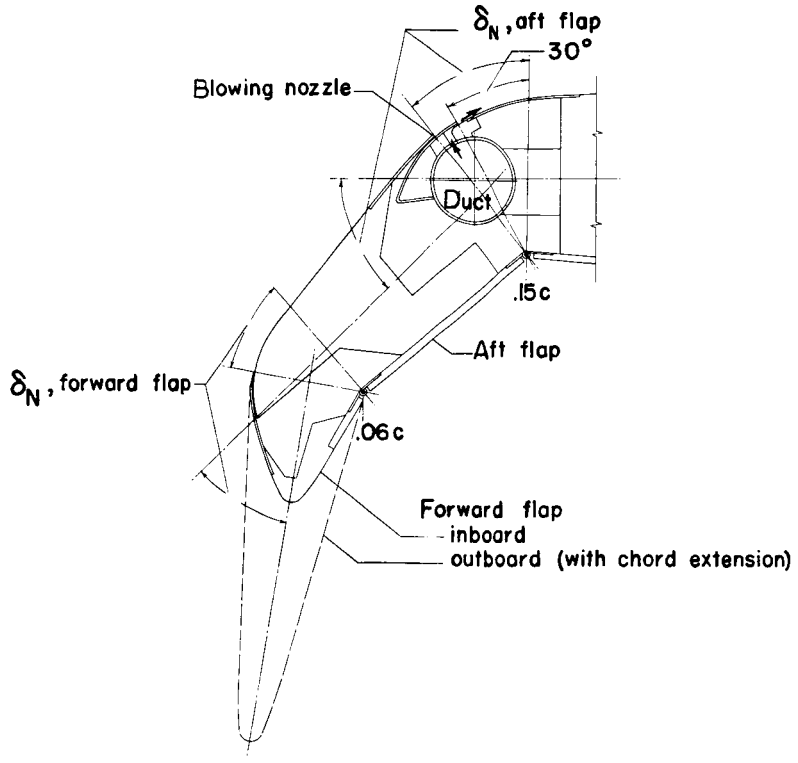

(a) Leading-edge flaps and blowing nozzle.

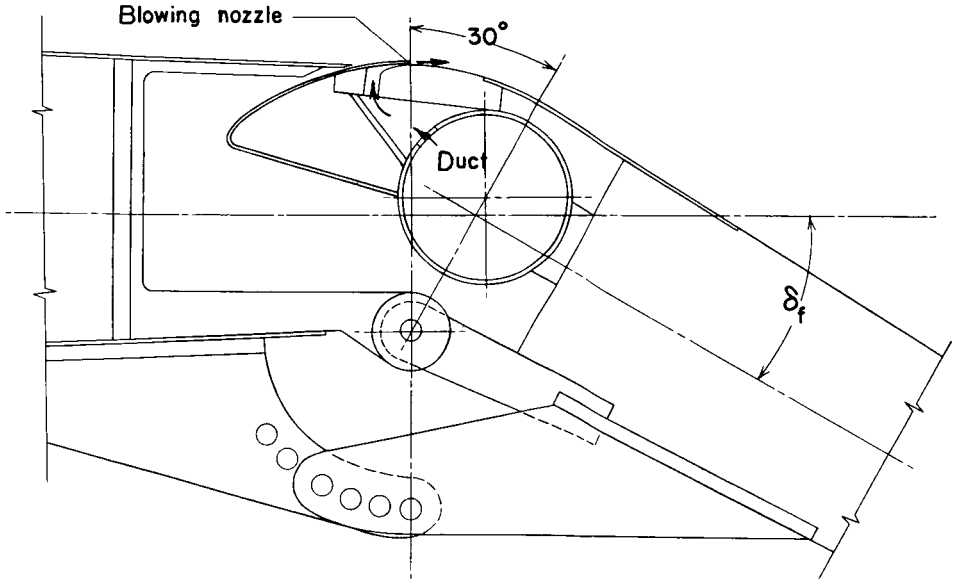

(b) Trailing-edge flap and blowing nozzle.

Figure 3.- Details of leading-edge and trailing-edge flaps and blowing nozzles.

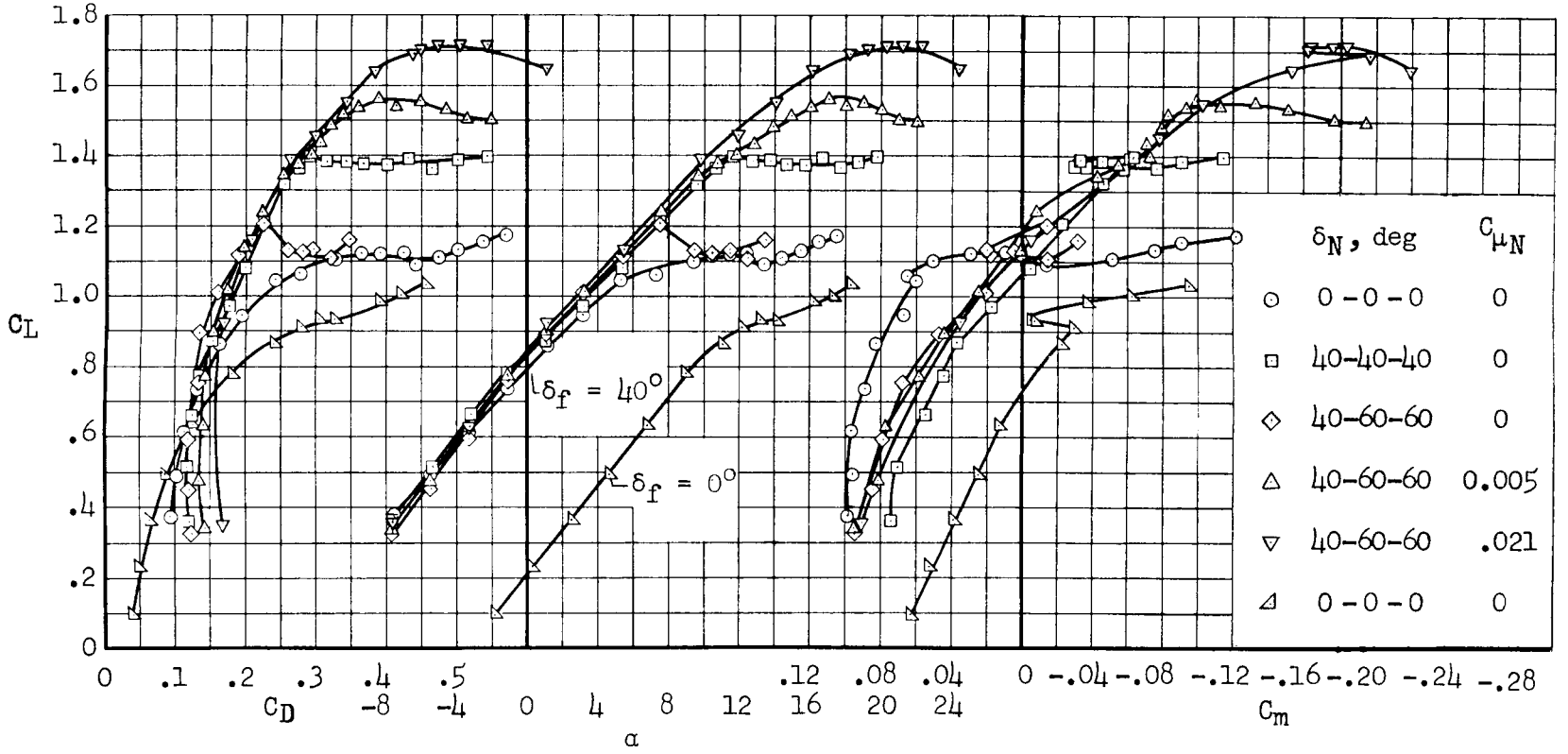

(a) $\delta_f = 40^\circ$ ($C_{\mu_f} = 0.009$) and 0°

Figure 4.- Aerodynamic characteristics of the model with various combinations of leading-edge and trailing-edge flap deflections and blowing BLC.

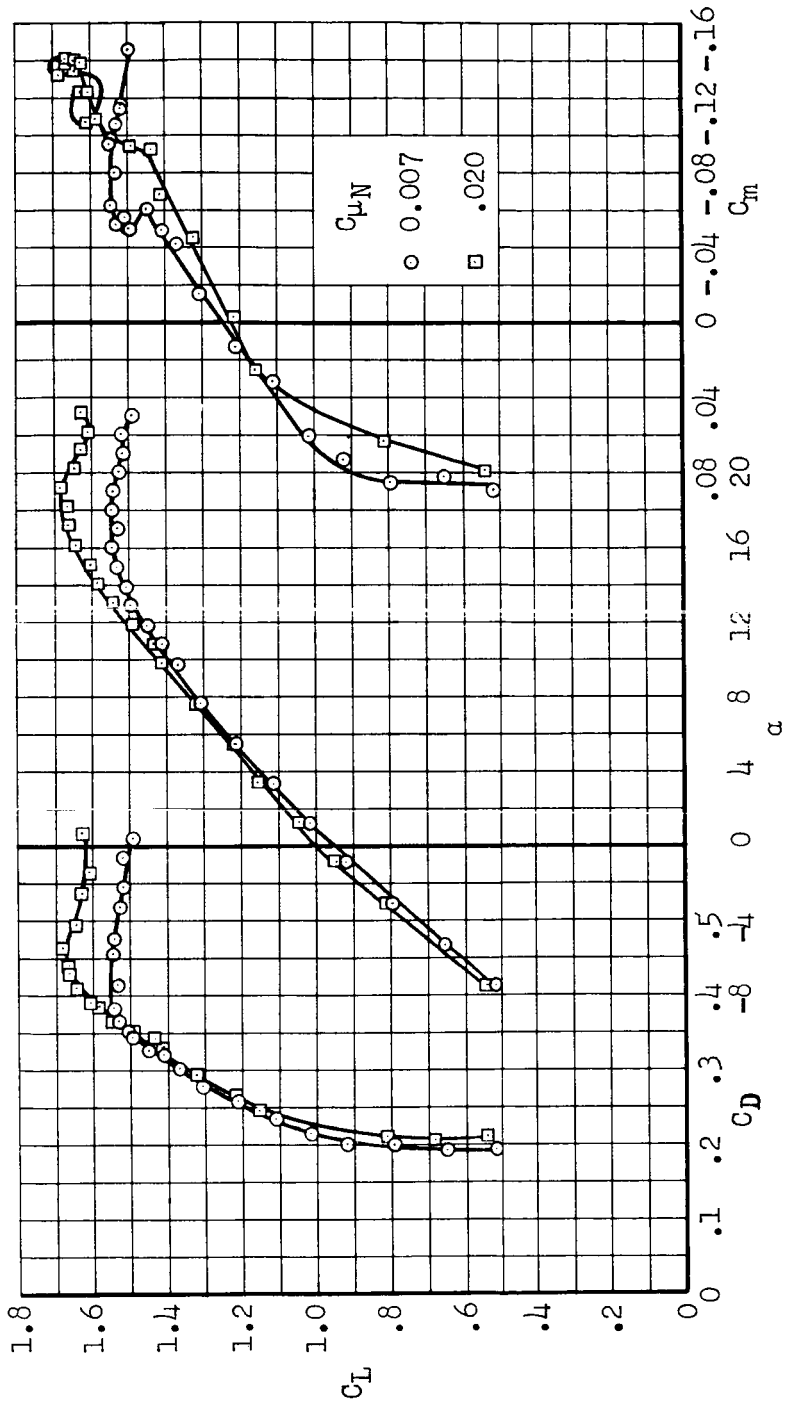

(b) δ_N = 40-60-60, δ_f = 55°, C_{μ_F} = 0.009

Figure 4.- Concluded.

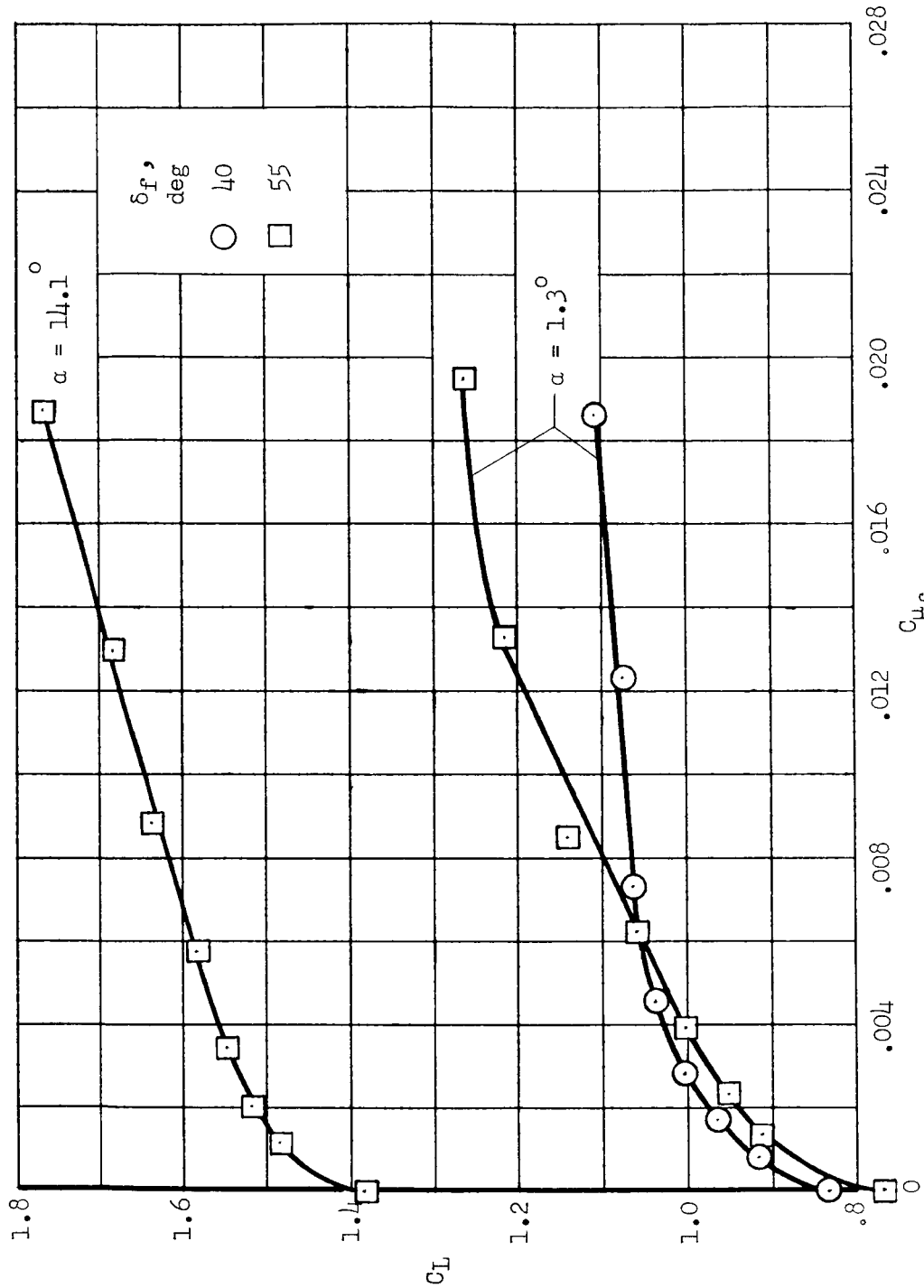

Figure 5.- Variation of lift with trailing-edge blowing flow coefficient; horizontal tail off; δ_N = 40-60-60, C_{μ_N} = 0.015.

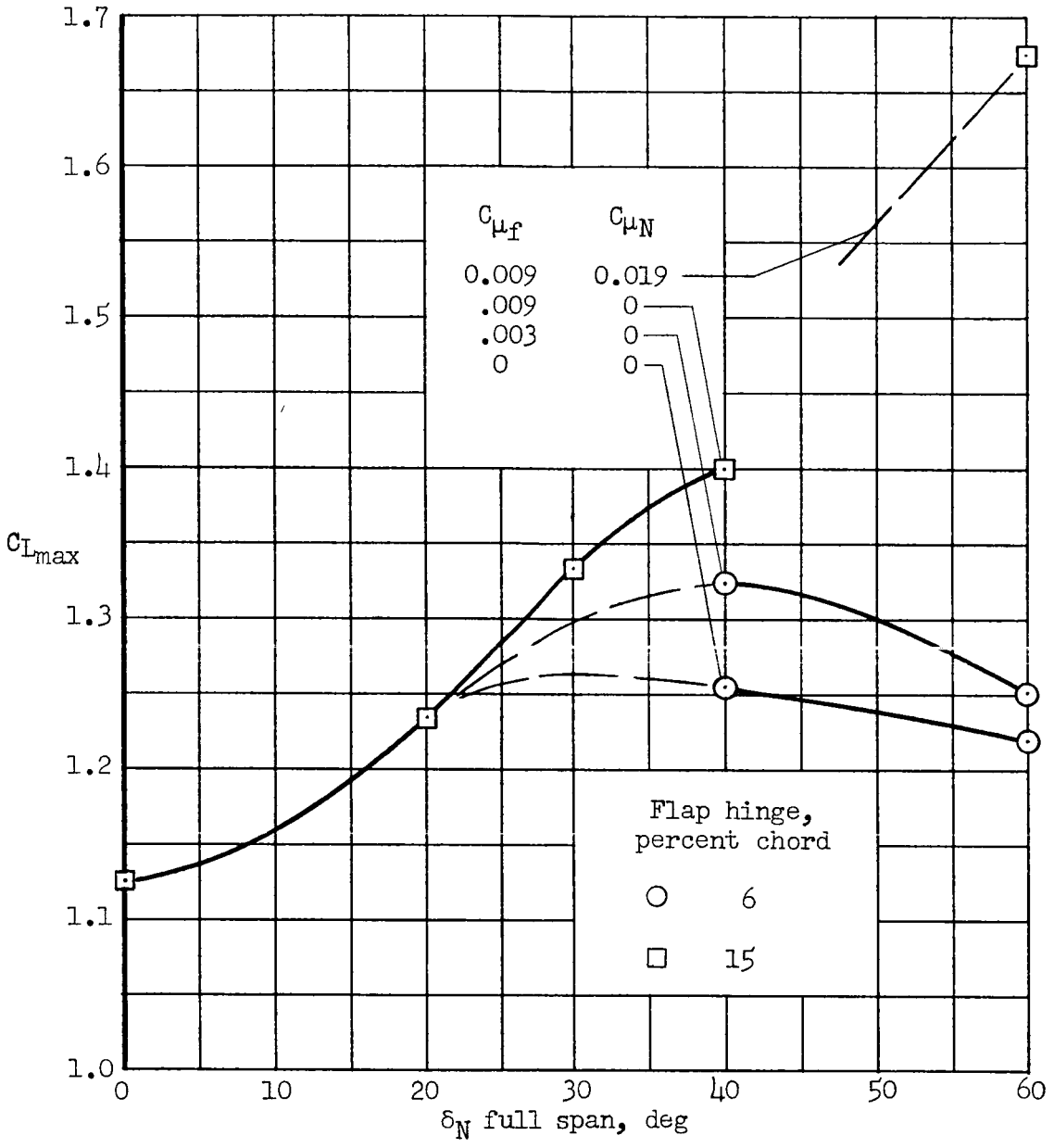

Figure 6.- Variation of maximum lift with full-span leading-edge flap deflection; with and without leading-edge and trailing-edge BLC; $\delta_f = 40^\circ$.

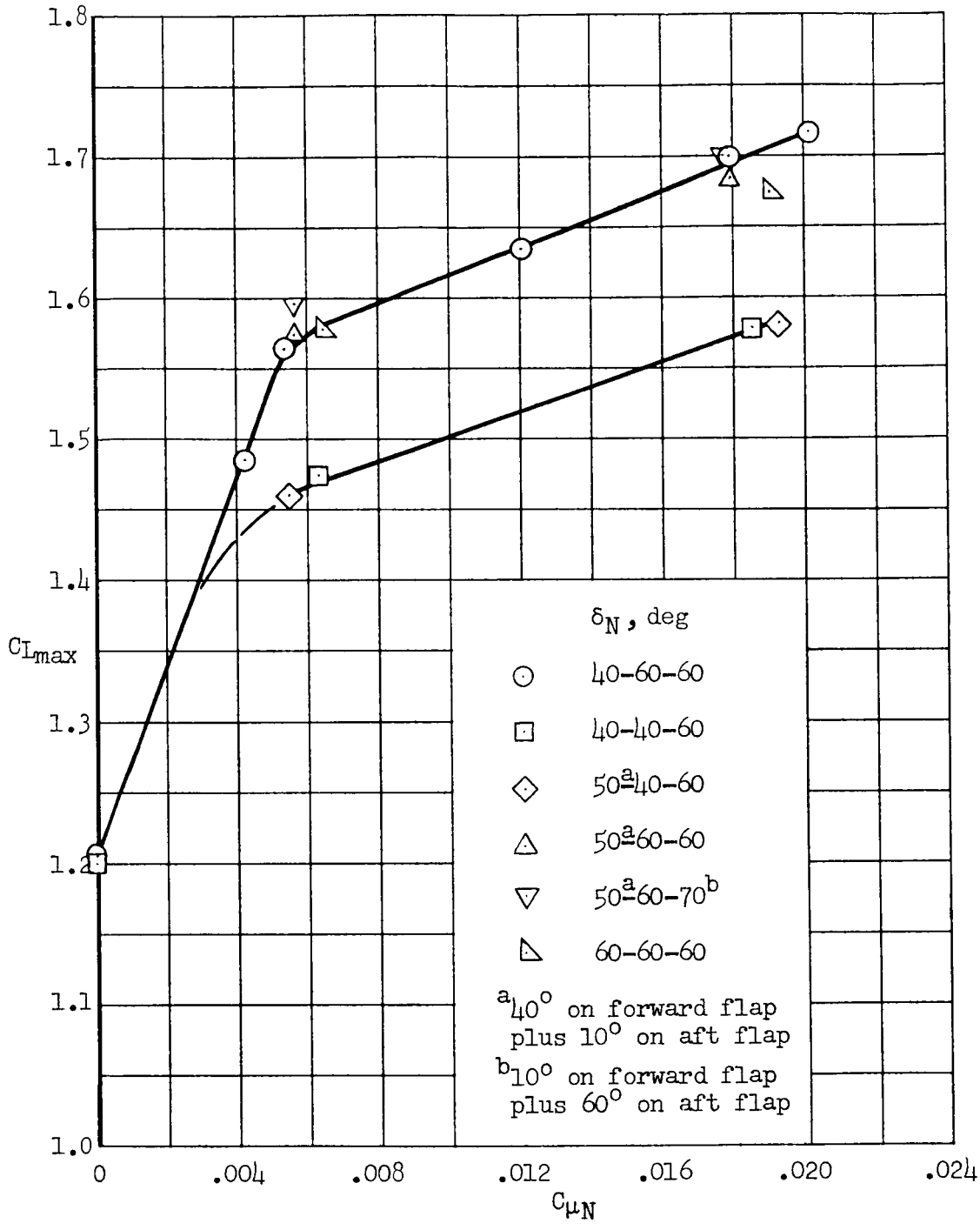

Figure 7.- Variation of maximum lift with leading-edge blowing flow coefficient for several leading-edge configurations; $\delta_f = 40°$, $C_{\mu_f} = 0.009$.

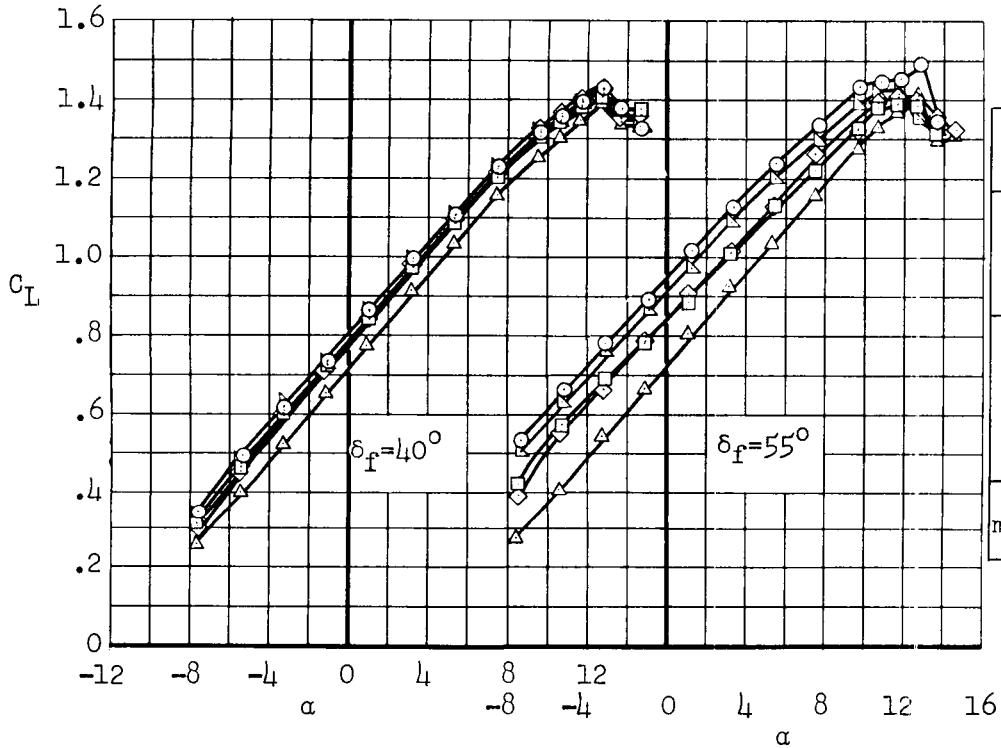

	Trailing-edge nozzle plugs and blockage				
	Plug length, inches				Percent nozzle blockage
△	1	1	1	1	3.4
□	3	3	3	3	10.3
◇		6	6		10.3
△	2.2	10.5	11.3	2.2	22.4
○	None				
2y/b to middle of plug	.18	.22	.46	.57	

Figure 8.- Effects of trailing-edge nozzle blockage on lift without leading-edge BLC; δ_N forward flap = 40° (full span); δ_N aft flap = 10° (inboard and middle segments) and 20° (outboard segment); C_{μ_f} = 0.008.

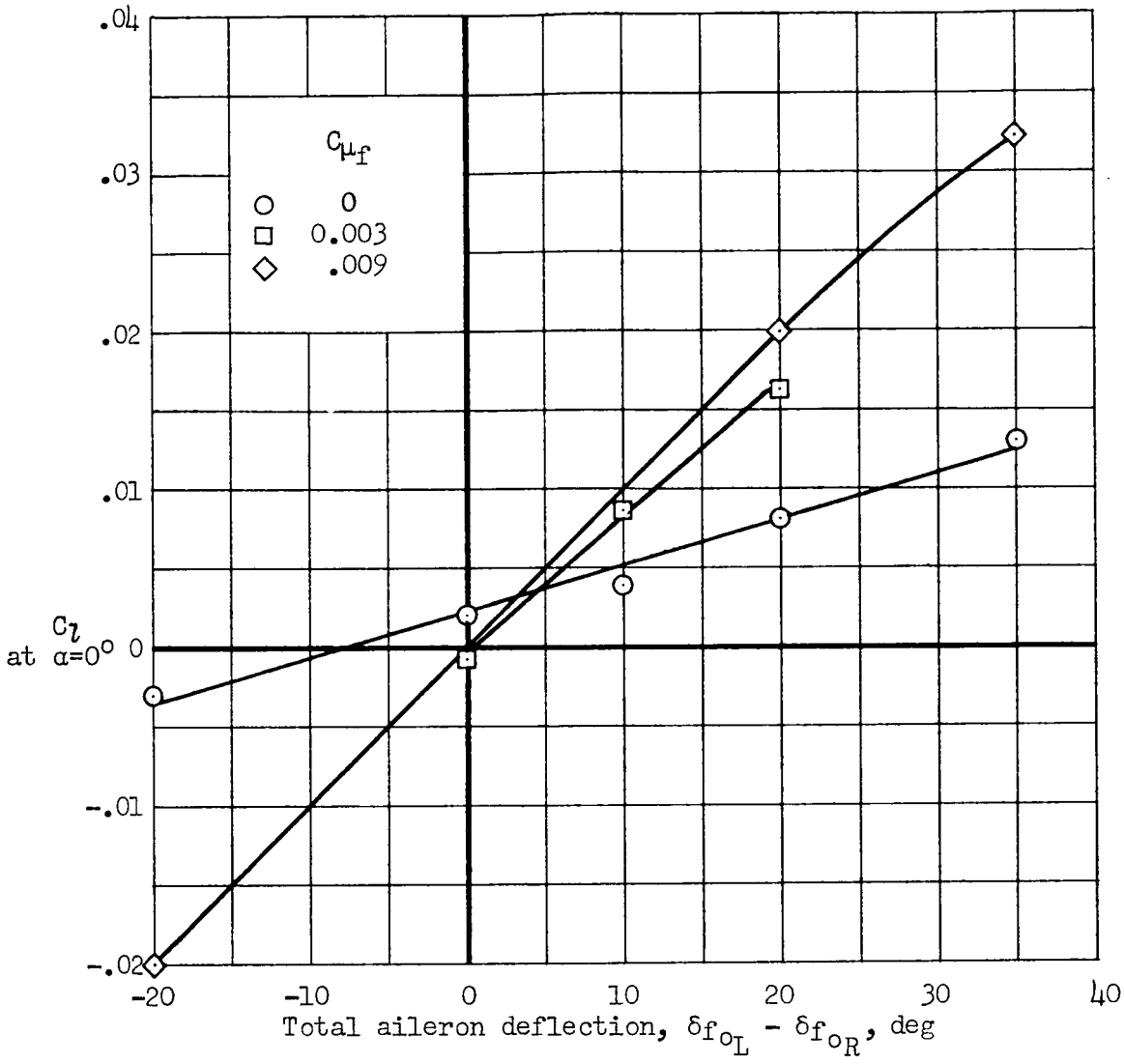

Figure 9.- Variation of rolling-moment coefficient with aileron deflection; δ_N forward flap = 40° (full span); δ_N aft flap = 10° (inboard and middle segments) and 20° (outboard segment); δ_{f_i} = 40°, $(\delta_{f_{o_L}} + \delta_{f_{o_R}})/2$ = 40°.

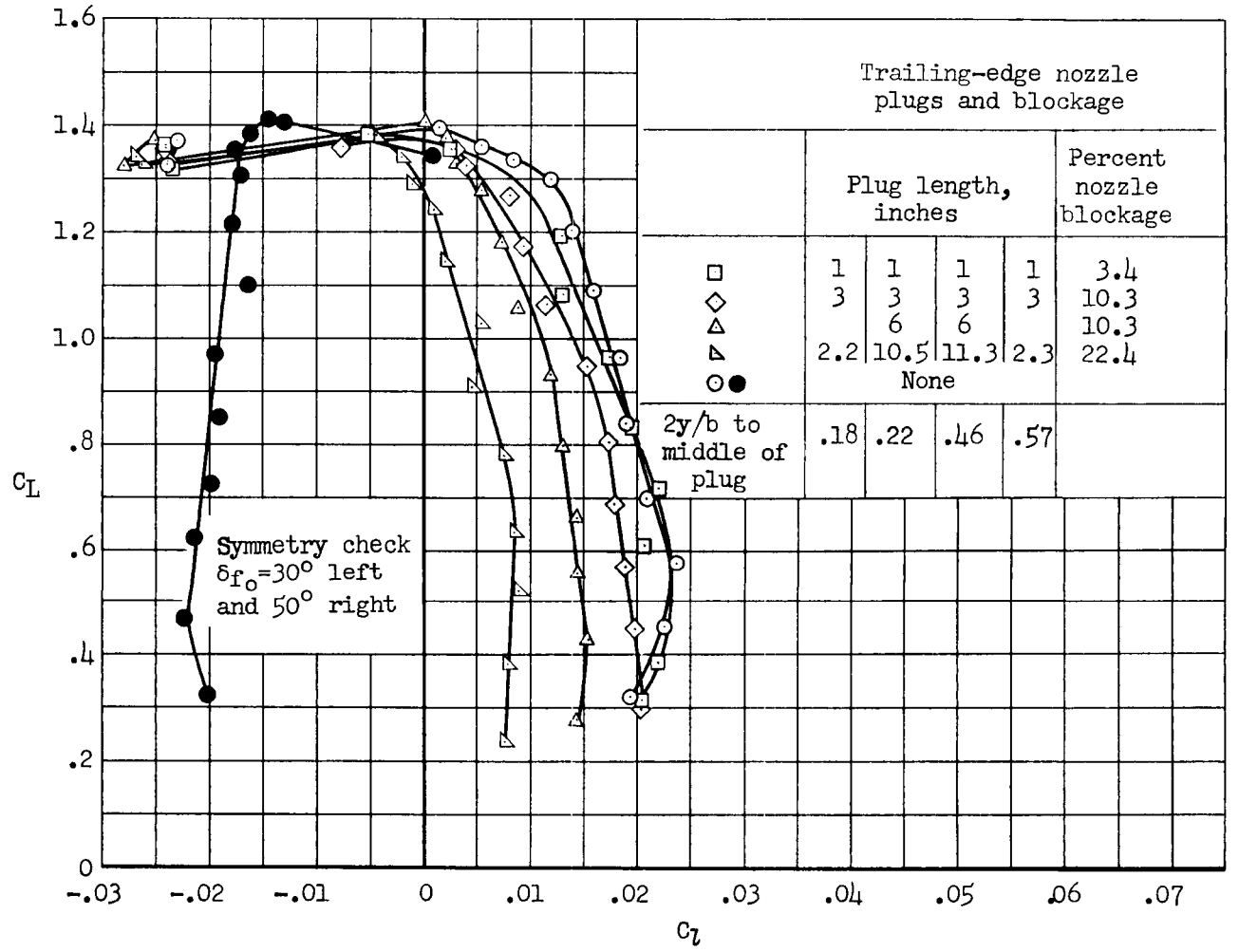

Figure 10.- Effects of trailing-edge nozzle blockage on aileron effectiveness in roll control without leading-edge BLC; δ_N forward flap = 40° (full span); δ_N aft flap = 10° (inboard and middle segments) and 20° (outboard segment); $\delta_{f_{o_L}}$ = 50°, $\delta_{f_{o_R}}$ = 30°, C_{μ_f} = 0.008.

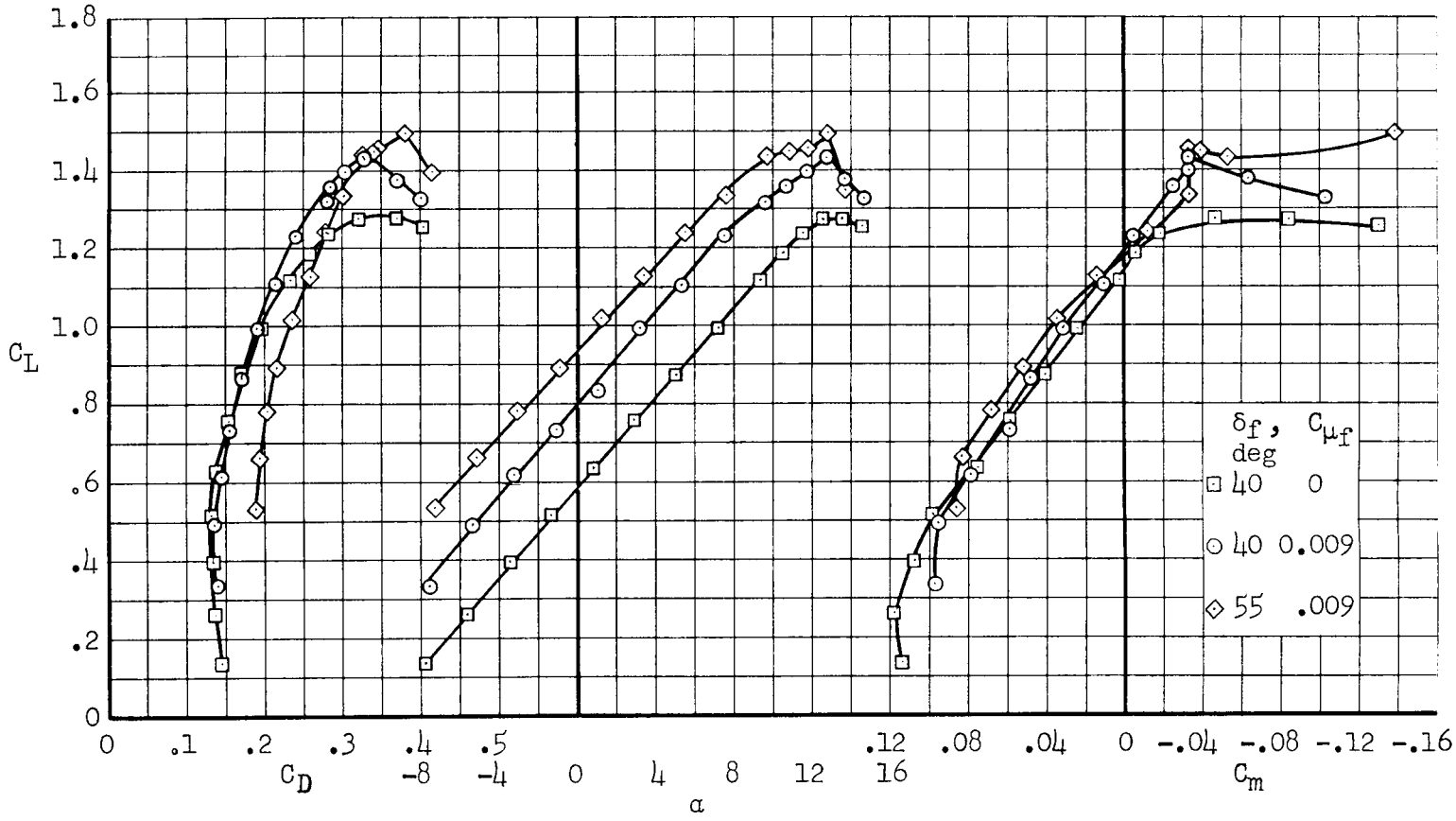

Figure 11.- Aerodynamic characteristics of the model with double-droop leading-edge flaps deflected without BLC and trailing-edge flaps deflected with and without BLC; δ_N forward flap = 40° (full span); δ_N aft flap = 10° (inboard and middle segments) and 20° (outboard segment).

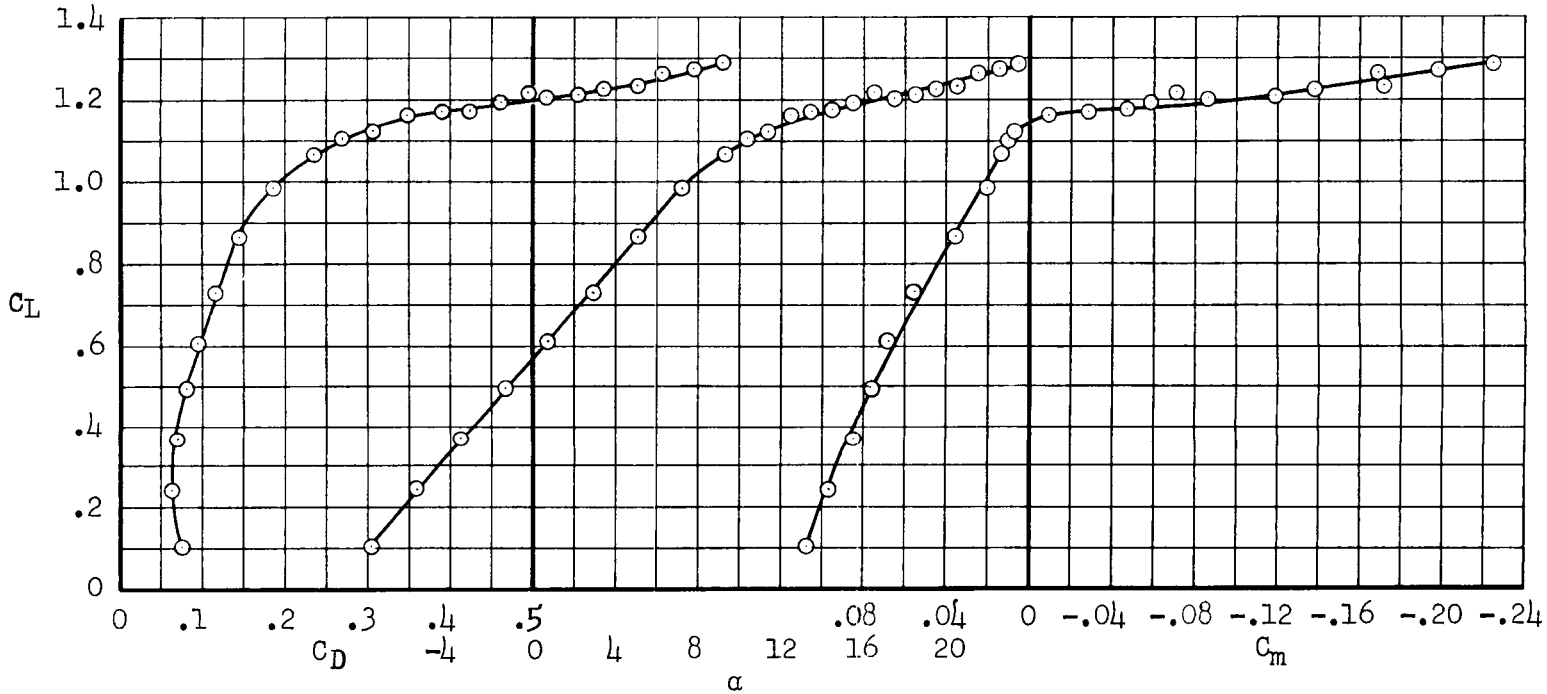

Figure 12.- Aerodynamic characteristics of the model with single-droop leading-edge flaps deflected without BLC and with the wing at 7° of incidence and trailing-edge flaps deflected without BLC; δ_N = 25-25-27, δ_f = 20°.

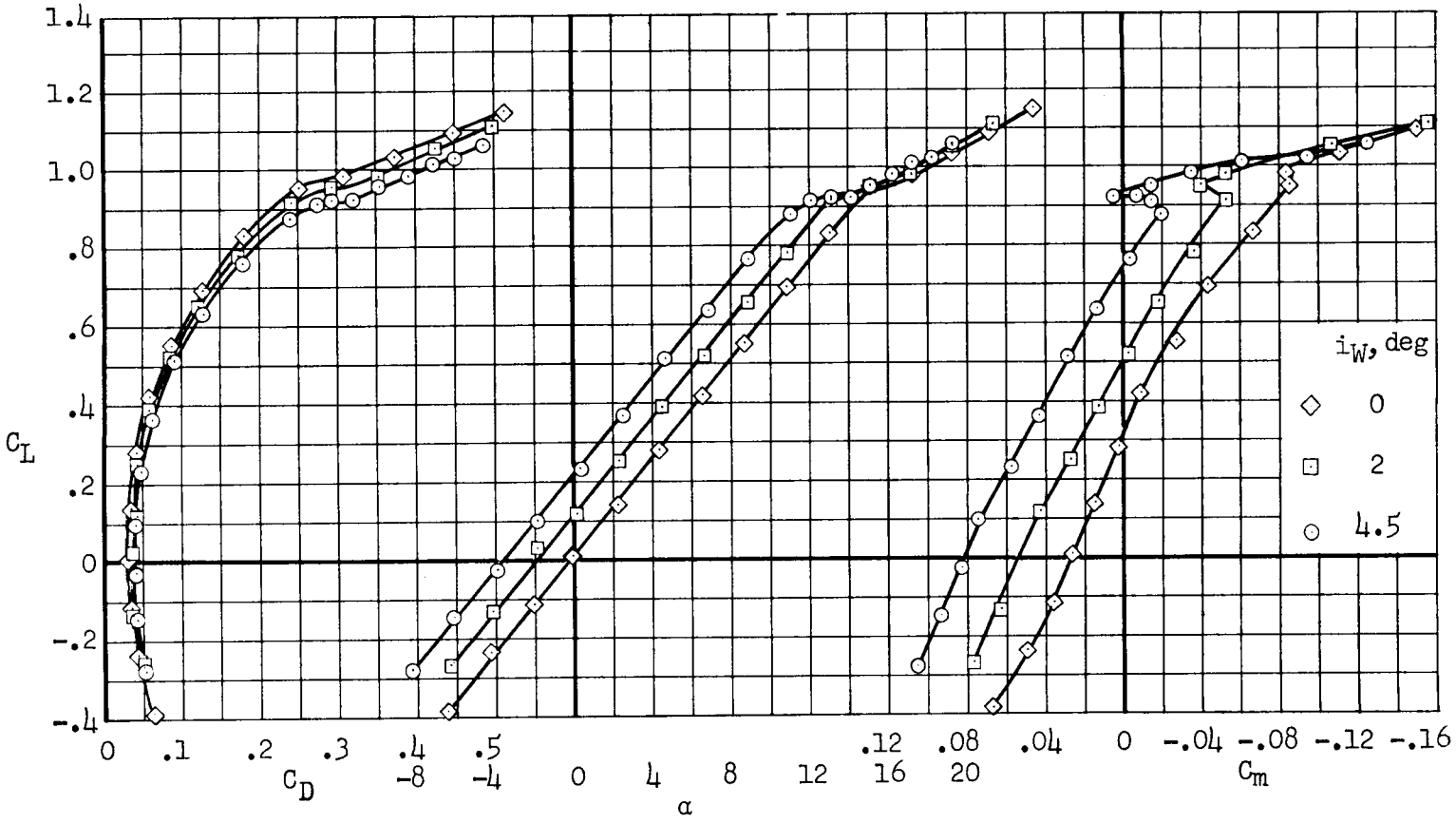

Figure 13.- Effect of wing incidence on the aerodynamic characteristics of the model with leading-edge and trailing-edge flaps undeflected; $i_t = 0^\circ$.

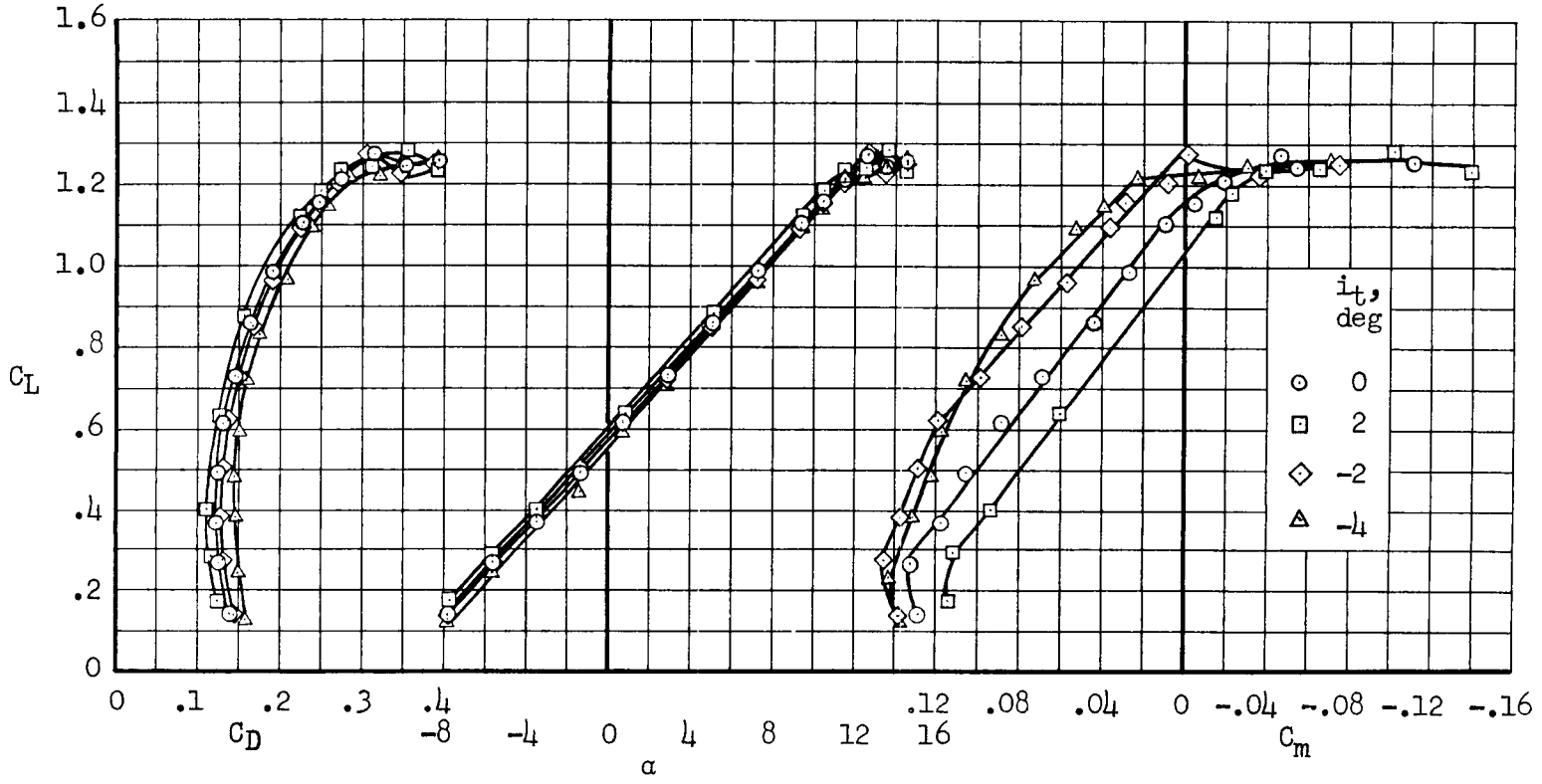

Figure 14.- Effect of tail incidence on the aerodynamic characteristics of the model with double-droop leading-edge flaps and trailing-edge flaps deflected without BLC; δ_N forward flap = 40° (full span); δ_N aft flap = 10° (inboard and middle segments) and 20° (outboard segment); δ_f = 40°.